



Construction of mechanically durable superhydrophobic surfaces by thermal spray deposition and further surface modification



Xiuyong Chen, Yongfeng Gong, Xinkun Suo, Jing Huang, Yi Liu, Hua Li*

Key Laboratory of Marine Materials and Related Technologies, Zhejiang Key Laboratory of Marine Materials and Protective Technologies, Ningbo Institute of Materials Technology and Engineering, Chinese Academy of Sciences, Ningbo 315201, China

ARTICLE INFO

Article history:

Received 14 July 2015

Received in revised form 14 August 2015

Accepted 19 August 2015

Available online 20 August 2015

Keywords:

Superhydrophobicity

Thermal spraying

Polytetrafluoroethylene

Mechanical stability

ABSTRACT

Here we report a simple and cost-effective technical route for constructing superhydrophobic surfaces with excellent abrasion resistance on various substrates. Rough surface structures were fabricated by thermal spray deposition of a variety of inorganic materials, and further surface modification was made by applying a thin layer of polytetrafluoroethylene. Results show that the Al, Cu, or NiCrBSi coatings with the surface roughness of up to 13.8 μm offer rough surface profile to complement the topographical morphology in micro-/nano-scaled sizes, and the hydrophobic molecules facilitate the hydrophobicity. The contact angles of water droplets of $\sim 155^\circ$ with a sliding angle of up to 3.5° on the samples have been achieved. The newly constructed superhydrophobic coatings tolerate strong abrasion, giving clear insight into their long-term functional applications.

© 2015 Elsevier B.V. All rights reserved.

1. Introduction

Superhydrophobic surfaces with water contact angle (CA) greater than 150° and sliding angle (SA) lower than 10° have attracted extensive research attention from both scientific and industrial communities owing mainly to their potential applications [1,2], including self-cleaning [3], anti-corrosion [4], anti-fogging [5], microfluidic [6], anti-icing [7], anti-fouling [8], drag-reducing [9], etc. A variety of artificial superhydrophobic surfaces have been developed. Selection of appropriate processing approaches that offer the ease of fabrication and efficiency in cost is one of the major concerns. The construction of the surfaces by the emerging routes usually involves creating rough surface structures in the first place [10], followed by further modification with low surface energy materials such as fluorocarbons, fluoroalkylsilane and hydrophobic silica [11–13]. Many processing techniques for example lithography patterning [14], layer-by-layer deposition [15], anodic oxidation [16], electrodeposition [17], sol-gel [18], mold fabrication-hot embossing process [19], electrospinning and chemical vapor deposition [20] have been attempted for fabricating hydrophobic surfaces. Regardless of the success of the abovementioned methods, large-scale fabrication of the surfaces with sufficient mechanical strength yet remains elusive. In addition, most of

the nowadays methods are confined to specific materials. Searching appropriate techniques for making various engineering materials superhydrophobic with enhanced long-term stability is one of the current research goals. As one of the key surface techniques, thermal spray has been widely used to make coatings against wear, oxidation and corrosion together with other multifunctional purposes [21,22]. The technique offers the advantages of simplicity and cost-effective mass production of coatings of engineering materials on various substrates with desired microstructures [23].

In this study, we report a new technical route for constructing superhydrophobic metal surfaces on various substrates. The metal layer was deposited by thermal spray, followed by diffusion processing of low surface energy molecules (polytetrafluoroethylene, PTFE) into the porous coatings. By using this approach, the inorganic coating provides rough base structure, and the hydrophobic molecules facilitate the hydrophobicity. The newly constructed superhydrophobic coatings are durable against strong abrasion, showing long-term stability of superhydrophobicity. This research opens a new window for constructing superhydrophobic engineered surfaces for versatile applications.

2. Experimental setup

Commercial aluminum wire (Al, $\varnothing 2$ mm), copper powder (Cu, $-45 + 15 \mu\text{m}$), NiCrBSi powder (Ni60, $-75 + 15 \mu\text{m}$) were used as received (Beijing General Research Institute of Mining & Metallurgy, China). Polytetrafluoroethylene (PTFE, 60 wt.%, Aladdin

* Corresponding author.

E-mail address: lihua@nimte.ac.cn (H. Li).

Chemistry Co., China) was used for attaining the hydrophobicity. Several typical substrate materials, ceramic tile, glass, magnesium alloy (AZ91D), Cu, 316 stainless steel and titanium alloy (TC4) plates, were used for the coating deposition. Prior to the spraying, the substrates were surface grit blasted using 60 mesh black fused alumina sand. The high velocity arc spray (HVAS) system (TLAS-500C, China) was employed to deposit the Al coatings on the ceramic tile, glass, magnesium alloy (AZ91D), Cu, 316 stainless steel and titanium alloy (TC4) plates. For the arc spraying, the current and voltage of the arc were 100 A and 25 V respectively, and the standoff distance between the gun exit and substrate surface was 150 mm. Compressed air with the pressure of 0.5 MPa was used as auxiliary gas. Cu coatings were fabricated by flame spray (Wuhan Institute of Materials Protection, China) on 316 stainless steel plates. For the flame spraying, acetylene was used as the fuel gas with the flow rate of 25 l/min and working pressure of 0.1 MPa. Pressure and flow rate of oxygen were 0.5 MPa and 42 l/min respectively. The powder feed rate was 50 g/min and the spray distance was 150 mm. The APS-2000K plasma spray system (Beijing Aeronautical Manufacturing Institute, China) was used to deposit NiCrBSi coatings on 316 stainless steel plates. A net energy of 30 kW was used for the coating deposition. The primary gas and the powder carrier gas was argon with the flow rate of 42 l/min and 4 l/min, respectively. Hydrogen was used as the auxiliary gas (11 l/min). The powder feeding rate was 50 g/min and the spray distance was 120 mm. The coated samples were immersed in 5% PTFE solution at room temperature for 1 h, and then sintered for 2 h. For optimization purposes, the sintering temperatures, 25 °C, 100 °C, 150 °C, 200 °C, 250 °C, and 300 °C were attempted for making the PTFE layer.

Microstructure of the coatings was characterized by field emission scanning electron microscopy (FESEM, FEI Quanta FEG250, the Netherlands). Surface roughness of the coatings was measured by laser scanning confocal microscope (LSCM, Zeiss LSM 700, Germany). The water contact angle and slide angle values

were determined using a video-based optical system (Dataphysics OCA20, Germany) by measuring three samples for each type of the coatings and five points were tested for each sample. The chemical composition of the samples was investigated with a diffuse reflectance infrared Fourier transform spectroscopy (DRIFTS, model 6300, Bio-Rad Co. Ltd., USA). The mechanical stability of superhydrophobic samples was evaluated by scratch testing. The testing was carried out using 800 grit Al₂O₃ sandpapers as the abrasion surface. The superhydrophobic surfaces were tested facing the sandpaper surface with varying applied pressure and distance with a speed of 3 cm/s.

3. Results and discussion

The metallic coatings with rough surfaces were prepared via the three thermal spray processes. Their topographical morphologies and surface roughness are tunable as accomplished by using alternative thermal spray methods (Fig. 1a, c, and e). Micron-sized holes and micro-/nano-protuberances are clearly seen on the surfaces of the as-sprayed coatings, which are further clarified by the LSCM characterization (Fig. 2). The surface roughness as measured by LSCM shows the Ra value of 13.8 μm, 11.1 μm, and 8.9 μm for the Al coating, the Cu coating, and the Ni60 coating, respectively. The coatings provide in the first place the rough surface profile to complement the topographical morphology in micro-/nano-scaled sizes for various substrates to attain hydrophobicity. The rough nature of the coatings gives rise to extremely hydrophilic nature of their surfaces (Table 1). After modification with a very thin PTFE layer (Fig. 1b-1, d-1, and f-1), the surfaces displayed superhydrophobic properties with contact angles greater than 150°. However, the contact angle decreased with the increase of thickness of the PTFE layer. It is noted that the thick PTFE layer already completely covered the micro-/nano hybrid structures (Fig. 1b-2, d-2, and f-2), which could weaken the contribution of the base structure to the superhydrophobicity. Furthermore, it is noted that

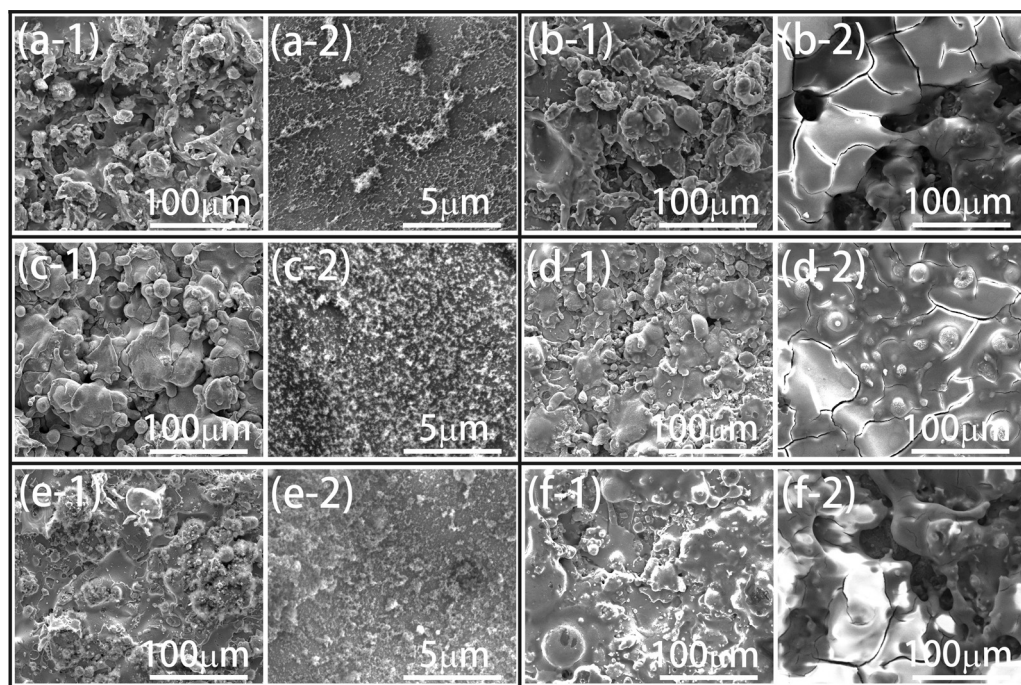


Fig. 1. SEM images of the coatings deposited on 316L substrates by various thermal spray approaches without (a, c, e) and with (b, d, f) the PTFE modification. (a, b) The Al coating deposited by high velocity arc spray, (c, d) the Cu coating deposited by flame spray, and (e, f) the Ni60 coating deposited by plasma spray. (a-2), (c-2), and (e-2) are enlarged views of selected area of (a-1), (c-1), and (e-1), respectively. (b-1), (d-1), and (f-1) are the coatings with a very thin PTFE top layer, and (b-2), (d-2), and (f-2) are the coatings with a thick PTFE top layer.

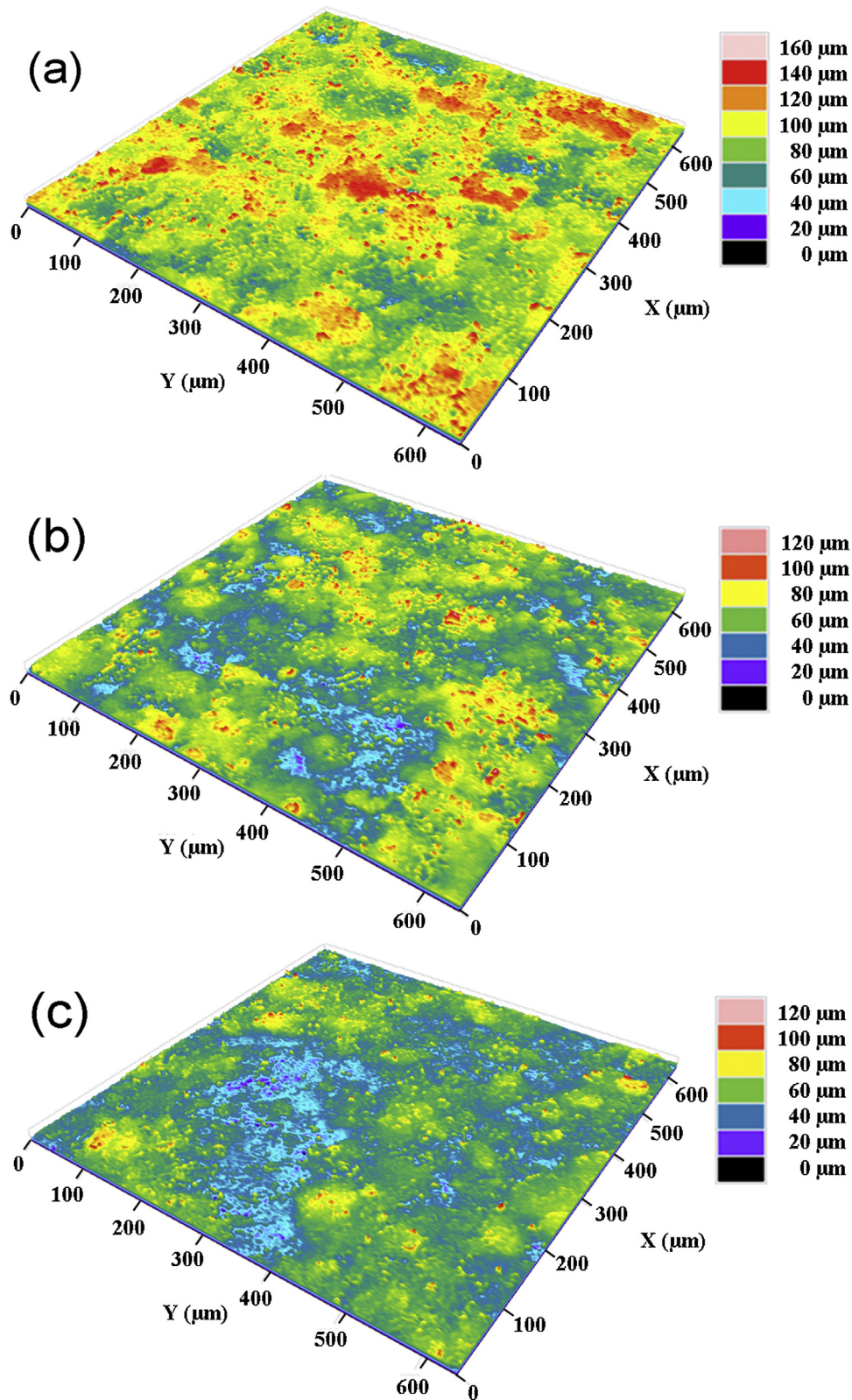


Fig. 2. Surface profile of (a) the Al coating, (b) the Cu coating, and (c) the Ni60 coating, the roughness of the coatings were measured by laser scanning confocal microscope.

the sintering temperature for PTFE plays crucial roles in making the hydrophobicity (Fig. 3). For the typical Al-PTFE coating on 316L plate, the sintering temperature of 25 $^{\circ}\text{C}$ results in hydrophilic feature of the coating with a water CA of $\sim 24^{\circ}$. CA increases with the increase in the sintering temperature. The coating attains

superhydrophobicity ($\sim 151^{\circ}$) after the sintering at 200 $^{\circ}\text{C}$. And there is a slight increase in CA after the sintering at 250 $^{\circ}\text{C}$, but no significant increase in CA is seen after the sintering at 300 $^{\circ}\text{C}$. The temperature of 250 $^{\circ}\text{C}$ was therefore selected for the treatment of all the coating samples. After the modification by PTFE, CA

Table 1
Contact angle and sliding angle of water droplets on the coatings with/without the PTFE modification.

Samples	Contact angle (°)	Sliding angle (°)
Al coating	0	–
Al coating-PTFE	152.5	3.5
Cu coating	62	–
Cu coating-PTFE	151	7.0
NiCrBSi coating	26	–
NiCrBSi coating-PTFE	150	8.5

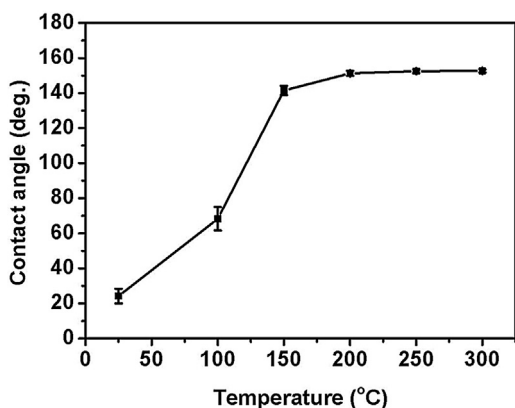


Fig. 3. Variation of water contact angle of the Al-PTFE coating on 316L plate with sintering temperature.

measured at room temperature increased sharply to the value greater than 150° and SA turns to be less than 10° for all the coatings (Al, Cu, and Ni60). The contact angles and sliding angles of water droplets on the surfaces of the samples are listed in Table 1. This suggests the superhydrophobic nature of the treated surfaces. It is worth to notice that CA of pure smooth PTFE surface is $\sim 120^\circ$, much lower than the CA observed in this study. This indicates a synergistic effect achieved by both the pre-constructed rough structure and the low surface energy PTFE. Moreover, thermal sprayed coatings virtually possess certain amount of porosity, low surface energy molecules can therefore easily diffuse into and colonize inside the pores within the coatings. This offers the advantages of preventing effectively the loss of PTFE, in turn giving rise to enhanced service duration of the surfaces under strong abrasion conditions [24–26].

To clarify the effect of sintering temperature on the surface chemistry of the coatings, the sintering temperature of 20°C and 250°C were typically investigated. The modification of the coatings with PTFE was confirmed by DRIFTS (Fig. 4). The intense peak

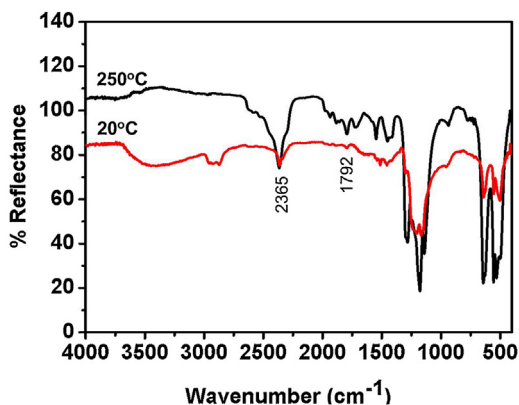


Fig. 4. DRIFTS spectra detected from the superhydrophobic surfaces of the treated 316 stainless steel samples after drying at 20°C and sintering at 250°C for 2 h.

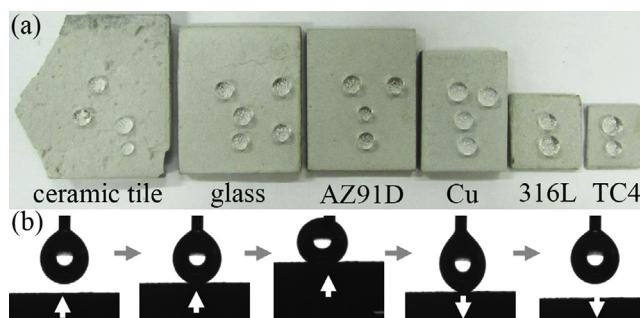


Fig. 5. Digital photos of (a) the water droplets standing on the superhydrophobic surfaces of the coated substrates, and (b) the dynamic repelling of a water droplet by the superhydrophobic surfaces. The $5\ \mu\text{L}$ water droplet was hung at a syringe needle, showing extraordinary resistance to contacting the constructed surfaces. The white arrow points to the moving direction of the tested sample.

located at $1000\text{--}1500\ \text{cm}^{-1}$ is assigned to stretching vibration of a variety of CF_x species [27]. The band at $1792\ \text{cm}^{-1}$ refers to terminal double bonds ($-\text{CF}=\text{CF}_2-$) and the band at $2365\ \text{cm}^{-1}$ is attributed to a combination band of the two modes associated with the CF_2 backbone [28]. These peaks typically derived from PTFE are detected from the surfaces of both the coatings treated with the sintering temperature of 20°C and 250°C . This indicates that the PTFE layer remains intact even after the sintering at 250°C .

To investigate the possibility of constructing the superhydrophobic surfaces on various substrates, the typical materials, ceramic tile, glass, magnesium alloy (AZ91D), Cu, 316 stainless steel (316) and titanium alloy (TC4), have been used as the substrates in this study. The Al coatings were fabricated as the top rough layer on these substrates. Fig. 5a shows the photographs of the water droplets standing on the superhydrophobic coatings. CA of the droplets on the samples ranges from 150° to 155° , which is likely attributed to the minor differences in the surface roughness of the Al coatings. The adhesion between the superhydrophobic surface and water droplet was assessed according to an established method [29]. It is clear that the water droplet hung at the needle tip of the syringe is difficult to be pulled down to the superhydrophobic surface, even after tight compression and severe deformation (Fig. 5b). It is suggested that the adhesive force between the water droplet and the superhydrophobic surface is extremely feeble.

The mechanical durability of the superhydrophobic surfaces was evaluated by scratch testing, which has been used for measuring the mechanical abrasion resistance of superhydrophobic surfaces [30–34]. This approach could be appropriate for assessing the anti-abrasion performances of superhydrophobic surfaces, largely due to the fact that the surfaces are rarely used under severe wear conditions. In this study, the scratch testing was carried out using 800 grit Al_2O_3 sandpaper as the abrasion surface, as illustrated in Fig. 6a. The superhydrophobic surfaces facing the sandpaper were tested with a sliding speed of $3\ \text{cm/s}$ under varied sliding distance and applied pressure. The sliding was repeated against the same surface length to achieve the total distance as a sum. The evolution of CA of the water droplets on the superhydrophobic surfaces versus the abrasion length is shown in Fig. 6b. The contact angle decreased with the increase of abrasion length under the pressure of $2.5\ \text{kPa}$. Surprisingly, the surface still retained the superhydrophobicity with a contact angle of 150° as the abrasion length was $1.0\ \text{m}$ under $2.5\ \text{kPa}$. After the abrasion for $0.5\ \text{m}$ under the pressure of $25\ \text{kPa}$, the hydrophobicity with a contact angle above 140° was still realized. The durability of the superhydrophobic coatings could be predominately attributed to the well-retained rough textures of the coating surfaces after the scratching (Fig. 6c and d). It

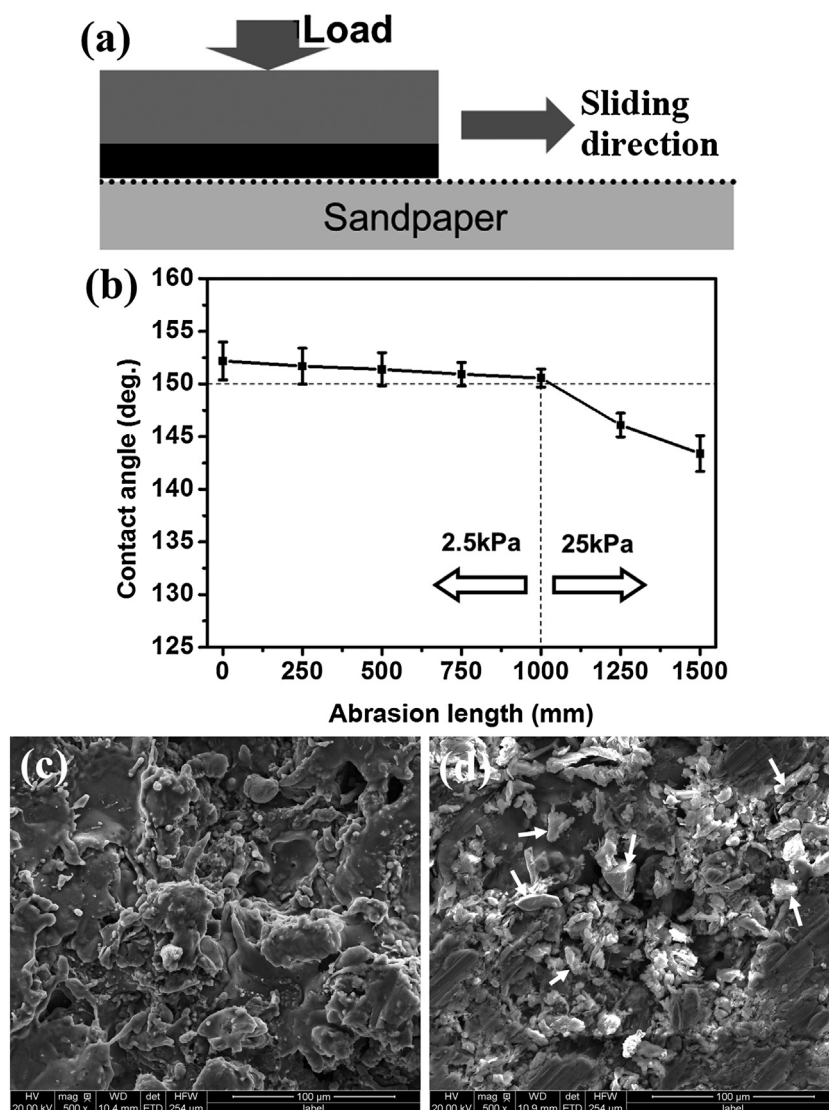


Fig. 6. (a) Schematic illustration of the scratch testing for evaluating the mechanical durability of the superhydrophobic surfaces, (b) contact angle of the superhydrophobic surface versus the abrasion length under the applied pressure of 2.5 kPa and 25 kPa, and (c, d) SEM images of the superhydrophobic surfaces before (c) and after (d) the abrasion for 1.0 m at 2.5 kPa and following 0.5 m at 25 kPa. Scale bars are 100 μm in (c, d). The white arrows in (d) point to the PTFE debris.

is believed that the metallic coating offers high strength to resist the abrasion. In addition, the porous structure already paves the way for the diffusion of the low surface energy molecules into the inside of the coatings. In fact, SEM analysis already disclosed the PTFE debris, which was likely pulled out by the abrasion from the coatings (Fig. 6d). The mechanical strength of the coatings and the presence of PTFE inside the coatings contribute to the continuation of the low surface energy hydrophobic layer and the long-lived superhydrophobicity.

4. Conclusions

In summary, superhydrophobic inorganic/organic composite coatings were constructed by a simple and new strategy for long-term functional services. Vast materials can be coated on engineering materials by thermal spray deposition of metals/ceramics/composites and following additional modification using low surface energy molecules. The results open a new window for cost-effective large-scale fabrication of superhydrophobic surfaces on engineering structures for various applications.

Acknowledgements

This work was supported by National Natural Science Foundation of China (grant # 51401232, 41476064 and 31271017), China Postdoctoral Science Foundation (grant # 2014M551777) and Ningbo Municipal Nature Science Foundation (grant # 2014A610005).

References

- [1] S. Wang, L. Jiang, Definition of superhydrophobic states, *Adv. Mater.* 19 (2007) 3423–3424.
- [2] X. Zhang, F. Shi, J. Niu, Y. Jiang, Z. Wang, Superhydrophobic surfaces: from structural control to functional application, *J. Mater. Chem.* 18 (2008) 621–633.
- [3] F. Wang, T. Shen, C. Li, W. Li, G. Yan, Low temperature self-cleaning properties of superhydrophobic surfaces, *Appl. Surf. Sci.* 317 (2014) 1107–1112.
- [4] J. Zhang, Z. Kang, Effect of different liquid–solid contact models on the corrosion resistance of superhydrophobic magnesium surfaces, *Corros. Sci.* 87 (2014) 452–459.
- [5] Y. Lai, Y. Tang, J. Gong, D. Gong, L. Chi, C. Lin, Z. Chen, Transparent superhydrophobic/superhydrophilic TiO₂-based coatings for self-cleaning and anti-fogging, *J. Mater. Chem.* 22 (2012) 7420–7426.

- [6] M. Elsharkawy, T.M. Schutzius, C.M. Megaridis, Inkjet patterned superhydrophobic paper for open-air surface microfluidic devices, *Lab Chip* 14 (2014) 1168–1175.
- [7] R. Liao, Z. Zuo, C. Guo, Y. Yuan, A. Zhuang, Fabrication of superhydrophobic surface on aluminum by continuous chemical etching and its anti-icing property, *Appl. Surf. Sci.* 317 (2014) 701–709.
- [8] J. Genzer, K. Efimenko, Recent developments in superhydrophobic surfaces and their relevance to marine fouling: a review, *Biofouling* 22 (2006) 339–360.
- [9] C. Lee, C.J. Kim, Underwater restoration and retention of gases on superhydrophobic surfaces for drag reduction, *Phys. Rev. Lett.* 106 (2011) 014502.
- [10] P.N. Manoudis, I. Karapanagiotis, A. Tsakalof, I. Zuburtikudis, C. Panayiotou, Superhydrophobic composite films produced on various substrates, *Langmuir* 24 (2008) 11225–11232.
- [11] H. Zhou, H. Wang, H. Niu, A. Gestos, X. Wang, T. Lin, Fluoroalkyl silane modified silicone rubber/nanoparticle composite: a super durable, robust superhydrophobic fabric coating, *Adv. Mater.* 24 (2012) 2409–2412.
- [12] X. Li, J. Shen, A facile two-step dipping process based on two silica systems for a superhydrophobic surface, *Chem. Commun.* 47 (2011) 10761–10763.
- [13] J. Wang, X. Song, R. Li, J. Shen, G. Yang, H. Huang, Fluorocarbon thin film with superhydrophobic property prepared by pyrolysis of hexafluoropropylene oxide, *Appl. Surf. Sci.* 258 (2012) 9782–9785.
- [14] J. Feng, M.T. Tuominen, J.P. Rothstein, Hierarchical superhydrophobic surfaces fabricated by dual-scale electron-beam-lithography with well-ordered secondary nanostructures, *Adv. Funct. Mater.* 21 (2011) 3715–3722.
- [15] Y. Zhao, Z. Xu, X. Wang, T. Lin, Superhydrophobic and UV-blocking cotton fabrics prepared by layer-by-layer assembly of organic UV absorber intercalated layered double hydroxides, *Appl. Surf. Sci.* 286 (2013) 364–370.
- [16] C. Jeong, C.H. Choi, Single-step direct fabrication of pillar-on-pore hybrid nanostructures in anodizing aluminum for superior superhydrophobic efficiency, *ACS Appl. Mater. Interfaces* 4 (2012) 842–848.
- [17] L. Hao, Z. Chen, R. Wang, C. Guo, P. Zhang, S. Pang, A non-aqueous electrodeposition process for fabrication of superhydrophobic surface with hierarchical micro/nano structure, *Appl. Surf. Sci.* 258 (2012) 8970–8973.
- [18] S.A. Mahadik, M.S. Kavale, S.K. Mukherjee, A.V. Rao, Transparent superhydrophobic silica coatings on glass by sol-gel method, *Appl. Surf. Sci.* 257 (2010) 333–339.
- [19] S.E. Lee, K.W. Lee, J.H. Kim, K.C. Lee, S.S. Lee, S.U. Hong, Mass-producible superhydrophobic surfaces, *Chem. Commun.* 47 (2011) 12005–12007.
- [20] M.L. Ma, Y. Mao, M. Gupta, K.K. Gleason, G.C. Rutledge, Superhydrophobic fabrics produced by electrospinning and chemical vapor deposition, *Macromolecules* 38 (2005) 9742–9748.
- [21] W.H. Liu, F.S. Shieu, W.T. Hsiao, Enhancement of wear and corrosion resistance of iron-based hard coatings deposited by high-velocity oxygen fuel (HVOF) thermal spraying, *Surf. Coat. Technol.* 249 (2014) 24–41.
- [22] C.U. Hardwicke, Y.C. Lau, Advances in thermal spray coatings for gas turbines and energy generation: a review, *J. Therm. Spray Technol.* 22 (2013) 564–576.
- [23] H. Herman, S. Sampath, R. McCune, Thermal spray: current status and future trends, *MRS Bull.* 25 (2000) 17–25.
- [24] T. Verho, C. Bower, P. Andrew, S. Franssila, O. Ikkala, R.H. Ras, Mechanically durable superhydrophobic surfaces, *Adv. Mater.* 23 (2011) 673–678.
- [25] E. Huovinen, L. Takkunen, T. Korpela, M. Suvanto, T.T. Pakkanen, T.A. Pakkanen, Mechanically robust superhydrophobic polymer surfaces based on protective micropillars, *Langmuir* 30 (2014) 1435–1443.
- [26] V. Kondrashov, J. Ruehe, Microcones and nanograss: toward mechanically robust superhydrophobic surfaces, *Langmuir* 30 (2014) 4342–4350.
- [27] V.N. Aderikha, V.A. Shapovalov, Mechanical and tribological behavior of PTFE-polyoxadiazole fiber composites. Effect of filler treatment, *Wear* 271 (2011) 970–976.
- [28] U. Lappan, U. Geissler, K. Lunkwitz, Electron beam irradiation of polytetrafluoroethylene in vacuum at elevated temperature: an infrared spectroscopic study, *J. Appl. Polym. Sci.* 74 (1999) 1571–1576.
- [29] X. Gao, X. Yao, L. Jiang, Effects of rugged nanoprotusions on the surface hydrophobicity and water adhesion of anisotropic micropatterns, *Langmuir* 23 (2007) 4886–4891.
- [30] F. Su, K. Yao, Facile fabrication of superhydrophobic surface with excellent mechanical abrasion and corrosion resistance on copper substrate by a novel method, *ACS Appl. Mater. Interfaces* 6 (2014) 8762–8770.
- [31] L. Yin, J. Yang, Y. Tang, L. Chen, C. Liu, H. Tang, C. Li, Mechanical durability of superhydrophobic and oleophobic copper meshes, *Appl. Surf. Sci.* 316 (2014) 259–263.
- [32] X. Zhu, Z. Zhang, J. Yang, X. Xu, X. Men, X. Zhou, Facile fabrication of a superhydrophobic fabric with mechanical stability and easy-repairability, *J. Colloid Interface Sci.* 380 (2012) 182–186.
- [33] Z. She, Q. Li, Z. Wang, L. Li, F. Chen, J. Zhou, Researching the fabrication of anticorrosion superhydrophobic surface on magnesium alloy and its mechanical stability and durability, *Chem. Eng. J.* 228 (2013) 415–424.
- [34] X. Zhu, Z. Zhang, X. Men, J. Yang, K. Wang, X. Xu, X. Zhou, Q. Xue, Robust superhydrophobic surfaces with mechanical durability and easy repairability, *J. Mater. Chem.* 21 (2011) 15793.